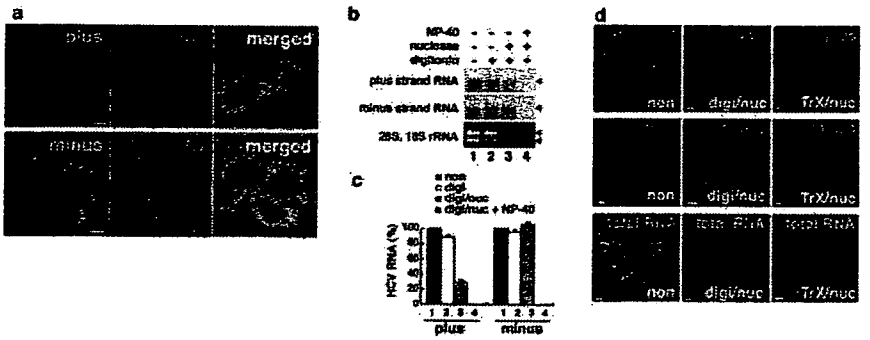

Supplementary Fig. S4 Kunitada Shimotohno
NCB-S11732B

Supplementary Fig. 4

Subcellular localizations of plus- and minus-strand HCV RNA

(a) JFH1^{E2FL} replicating cells were analyzed by *in situ* hybridization to detect plus- and minus-strand HCV RNA (green). The cells were also labeled with anti-PDI antibodies (red) and DAPI (blue). Scale bars = 10 μm. (b, c) Relative amounts of plus- and minus-strand HCV RNAs. JFH1^{E2FL}-expressing cells were permeabilized with digitonin. The cells were treated with nuclease in the presence or absence of NP-40. Then, total RNA was analyzed by Northern blots with strand-specific HCV RNA probes. 28S and 18S ribosomal RNA was stained with ethidium bromide (b). The signals were quantified and plotted in c (n = 3). The amounts of plus- and minus-strand RNA were similar before and after digitonin treatment (lanes 1 and 2). The level of plus-strand RNA, however, was reduced by approximately 70% after nuclease treatment, whereas the level of minus-strand RNA remained constant (lanes 2 and 3). Nuclease treatment in the presence of NP-40 used to lyse the membranes caused both plus- and minus-strand HCV RNA to disappear (lane 4). This result suggests that ~30% and ~100% of plus- and minus-strand HCV RNA, respectively, are located in the replication complexes. (d) Localization of nuclease-resistant JFH1^{E2FL} RNA was analyzed by *in situ* hybridization. Digitonin-permeabilized cells were treated with nuclease in the presence (TrX/nuc) or absence (digi/nuc) of Triton X-100. Total RNA was visualized with SYTO RNAselect. "non" indicates cells without digitonin and nuclease treatment. Using the nuclease-resistant HCV RNA as a marker of replication complexes, we examined the localization of the replication complexes. Both plus- and minus-strand HCV RNA were detected in the perinuclear region even after the nuclease treatment. As expected, these RNAs were no longer detectable after nuclease treatment in the presence of Triton X-100. The intensity of the plus-strand RNA signal decreased after nuclease treatment (compare upper left and middle panels). However, the intensity of the minus-strand RNA signal remained unchanged after the treatment. These results correlated with the data obtained by Northern blotting analysis. For this reason, the percentages of cells with overlapping signals for LDs and plus- or minus-strand HCV RNA (Fig. 2c) were measured after lysis of cells with digitonin and nuclease treatment. Scale bars = 10 μm.

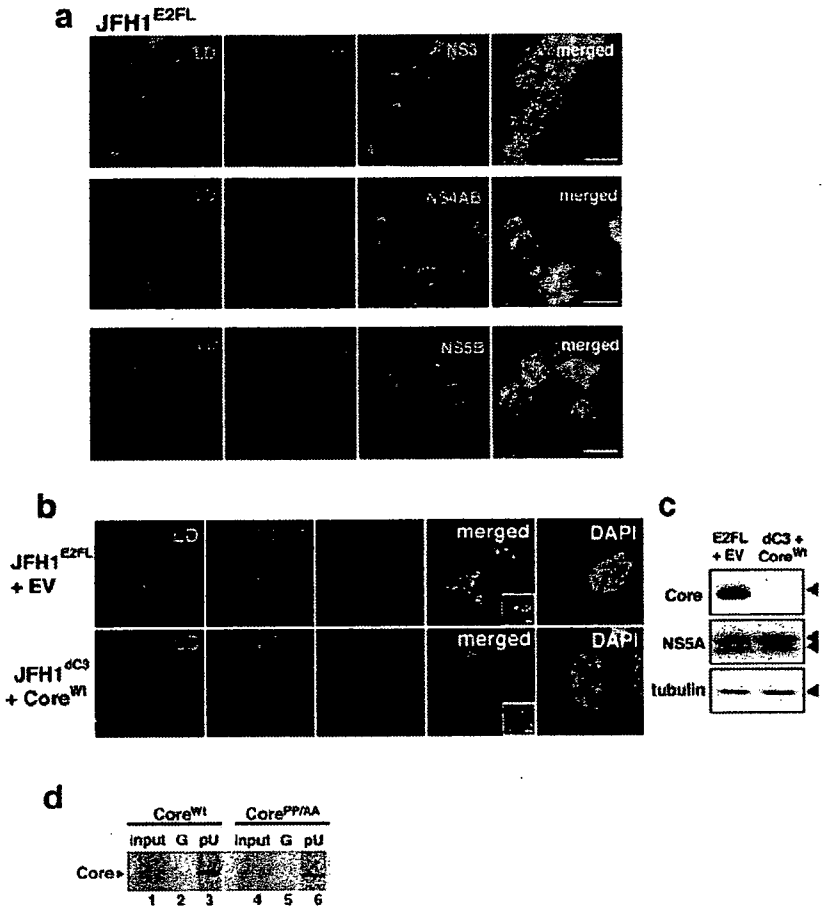

Supplementary Fig. S5 Kunitata Shimotohno NCB-S11732B

Supplementary Fig. 5

Subcellular localization of HCV proteins in JFH1^{E2FL}-replicating cells and cells inoculated with rescued viruses, and RNA binding nature of Core.

(a) JFH1^{E2FL}-replicating cells were labeled to detect LDs (green), Core (red), NS3 (cyan), NS4AB (cyan), and NS5B (cyan). Scale bars = 2 μm **(b)** The subcellular localizations of NS5A and Core in Huh-7.5 cells infected with viruses released from JFH1^{E2FL} replicon-bearings cells co-transfected with pcDNA3 (upper panels) and from JFH1^{dC3} replicon-bearing cells co-transfected with pcDNA3-Core^{Wt} (lower panels). Cells were labeled with DAPI (white), BODIPY 493/503 (green), anti-Core (blue), and anti-NS5A (red) antibodies. The insets are high magnifications of the corresponding panel. (c) HCV proteins from these infected cells were analyzed by western blotting. (d) An RNA-protein binding precipitation assay was performed with *in vitro*-translated and ^{35}S-radiolabeled Core^{Wt} (lane 1-3) and Core$^{PP/AA}$ (lane 4-6). The resulting precipitates were analyzed by SDS-PAGE and detected by autoradiography. "G" and "pU" mark samples obtained using protein G Sepharose and poly-U Sepharose as the resin, respectively. "input" indicates 1/20 of the amount of translated product used in this assay.

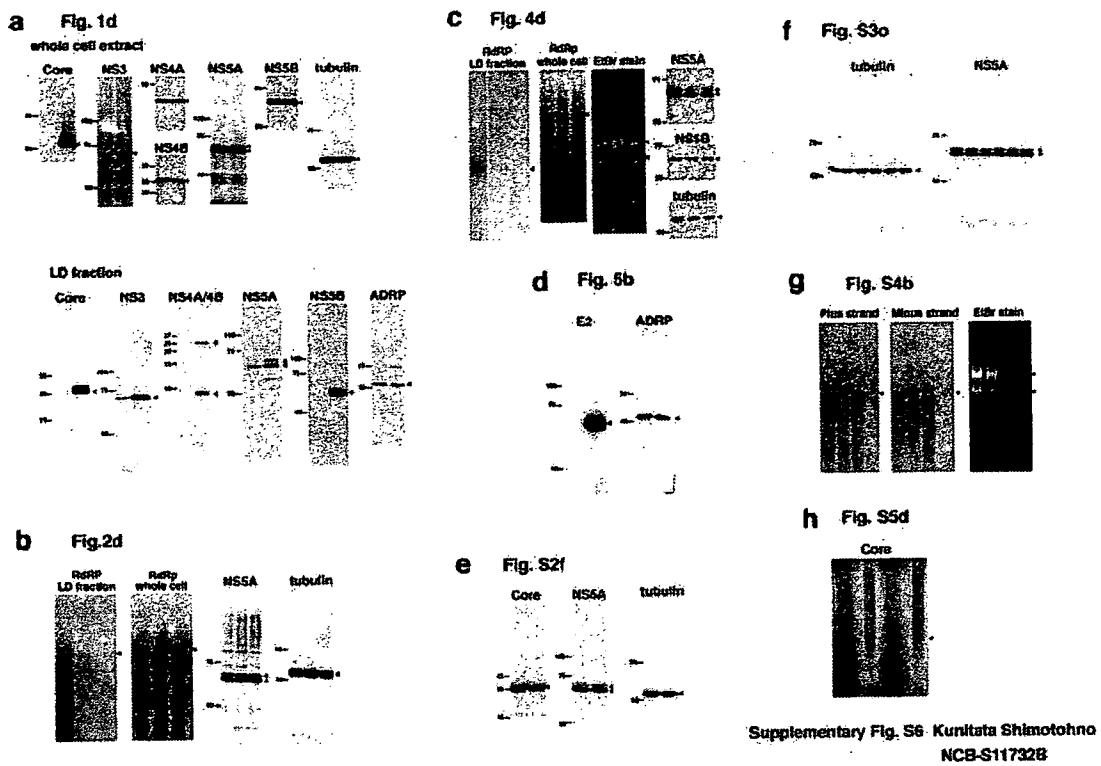

Supplementary Fig. 6

Full scan of key gel images depicted in the individual figures.

Full scans of (a) immunoblot detection of whole cell extract and LD fraction from JFH1^{E2FL}- and JFH1^{dC3}-replicating cells shown in Fig. 1d, (b) RNA synthesis assay and immunoblot detection of JFH1^{E2FL}-, JFH1^{dC3}-, and JFH1$^{PP/AA}$-replicating cells shown in Fig. 2d, (c) RNA synthesis assay and immunoblot detection of JFH1^{E2FL}-, JFH1^{AAA99}-, and JFH1^{AAA102}-replicating cells shown in Fig. 4d, (d) immunoblot detection of LD fraction from JFH1^{E2FL}- and JFH1^{dC3}-replicating cells shown in Fig. 5b, (e) immunoblot detection of JFH1^{E2FL}- and JFH1$^{PP/AA}$-replicating cells shown in Fig. S2f, (f) immunoblot detection of JFH1^{E2FL}-replicating cells shown in Fig. S3o, (g) Northern Blotting analysis of JFH1^{E2FL}-replicating cells shown in Fig. S4b, and (h) RNA-protein binding precipitation assay shown in Fig. S5d. Size of molecular weight markers (kDa) is indicated at the left side of western blot gel images. *In vitro* transcribed HCV RNA was used as a size marker for RNA gel electrophoresis (b, c, and g).

plasmid name	primer sequences (5' to 3')	template for PCR	restriction enzyme	original plasmid
pcDNA3-Core ^{1a1}	AGACCCAAGCTTCACCATGAGCACAAATCCTAAACC	pJFH1	HindIII	pcDNA3
	AATGGAATTCTCAAGCAGAGACCGGAACGGTGATGC		EcoRI	
pcDNA3-TME2	AGACCCAAGCTTCACCATGGGCTCACTGGGGCGTCATGTTC	pJFH1	HindIII	pcDNA3
	AATCCAATTCTCATCCTTCCGCCTCGCCCAACAAC		EcoRI	
pcDNA3-NS3	AGACCCAAGCTTCACCATGGGTGCCATCAGTGCTTATGCC	pJFH1	HindIII	pcDNA3
	AATGGAATTCTCAGGTCATGACCTCAAGGTCAGC		EcoRI	
pcDNA3-NS4B	AGACCCAAGCTTCACCATGGCCTCTAGGGCGGCTCTCATCG	pJFH1	HindIII	pcDNA3
	AATGGAATTCTCAGCATGGGATGGGGCAGTCCTC		EcoRI	
pcDNA3-NS5B	CTCGGATCCACCATGTCCATGTCATACTCCTGGACC	pJFH1	BamHI	pcDNA3
	AATGGAATTCCTACCGAGCGGGGAGTAGGAAGAGG		EcoRI	
pcDNA3-Core $^{PP/AA}$	CATGGGGTACATCGCCGTCGTAGGCGCCGCGCTTAGTGGCG	pJFH1 $^{PP/AA}$	HindIII	pcDNA3
	CGCCACTAAGCGCGGCGCCTACGACGGCGATGTACCCCATG		EcoRI	
pJFH1 ^{E2FL}	GATTACAAGGATGACGACGATAAGGGCGTGTTCAGCCATGGCCC	pJFH1	BsiWI	pJFH1
	CTTATCGTCGTCATCCTTGTAATCAACAGCGCCTCCAACCGTGG		NotI	
	GGGACATGATGATGAACTGG			
	GTAATGTCAAACACCACACC			
pJFH1 $^{4/4}$	GAAAAACCAAAAGAAACACCAACTATGCAACAGGGAACCTACC	pJFH1 ^{E2FL}	EcoRI	pJFH1 ^{E2FL}
	GTTGCTGTTTCTTTTGGTTTTTC		BsiWI	
	GGGACATGATGATGAACTGG			
	GTAATGTCAAACACCACACC			
pJFH1 $^{PP/AA}$	CATGGGGTACATCGCCGTCGTAGGCGCCGCGCTTAGTGGCG	pJFH1 ^{E2FL}	EcoRI	pJFH1 ^{E2FL}
	CGCCACTAAGCGCGGCGCCTACGACGGCGATGTACCCCATG		RsrII	
	GGGACATGATGATGAACTGG			
	GTAATGTCAAACACCACACC			
pJFH1 ^{E2FL} dBamHI	TACTGCCTGGCATCCTGTCTCC	pJFH1 ^{E2FL}	NsiI	pJFH1 ^{E2FL}
	GCAGACAGGATGCCAGGCAGTA		RsrII	
	CTATTACCAATGAGGTCAGC			
	GAACAATTTAGAGGTCAGCC			
pJFH1 $^{AAA/3}$	GGCCAGTGCGCGGCGGCACCCCCCACG	pJFH1 ^{E2FL}	BamHI	pJFH1 ^{E2FL} dBamHI
	CGTGCGCCGTCCCCCCCCCCACTGCCC		RsrII	
	TGGATGAACAGGCTTATTGC			
	GGTTGAAGCTCTACCTGATC			
pJFH1 $^{AAA/02}$	GCGCCGAAAGCCGCCGCGAACTACAAG	pJFH1 ^{E2FL}	BamHI	pJFH1 ^{E2FL} dBamHI
	CTTCTAGTTCCCCCCCCCTTTCCCCCC		RsrII	
	TGGATGAACAGGCTTATTGC			
	GGTTGAAGCTCTACCTGATC			

Supplementary Table

A list of the plasmids used in this work. The sets of primers used to amplify the target genes, the template plasmids used in the PCRs, the restriction sites, and plasmids into which the amplified DNA fragments were inserted are shown.

Supplementary Materials and Methods

Cell culture

The human hepatoma cell lines Huh-7 and Huh-7.5[1] were grown in Dulbecco's modified Eagle's medium (DMEM; Invitrogen, CA, USA) supplemented with 10% fetal bovine serum (FBS), 100 U/ml nonessential amino acids (Invitrogen), and 100 μg/ml penicillin and streptomycin sulfate (Invitrogen). Huh-7.5 cells were obtained from Dr. C. Rice. (Rockefeller University, USA)

Plasmid construction

All plasmids were generated by insertion of PCR-amplified fragments into expression plasmids. The plasmids, the primer sequences, templates for the PCRs, and the restriction enzyme sites used to construct the plasmids are listed in Supplementary Table 1.

DNA and RNA transfection

Transfection of HCV RNA was performed as previously described[2]. DNA transfection was performed using Lipofectamine 2000 (Invitrogen) according to the manufacturer's instructions.

Northern blotting

Northern blot analysis was performed as described previously[3] with strand specific RNA probes.

RT-PCR analysis

Quantitative real-time RT-PCR analysis of the HCV RNA titer was performed as described previously[4].

ELISA for the detection of Core

Core in the culture medium was quantified with an ELISA according to the manufacturer's protocol (HCV antigen ELISA test, Ortho-Clinical Diagnostics).

Thin-layer chromatography

Lipid samples extracted from cells were dissolved in chloroform methanol and were

subjected to thin-layer chromatography with a high-performance TLC plate (Merck) by the two-step method[5]. The plate was charred by a copper acetate phosphoric acid solution at 180°C.

***In vitro* transcription**

RNA for transfection was synthesized using MEGAscript T7 (Ambion, TX, USA). Plasmids carrying the JFH1 RNA sequence were linearized with *Xba*I and used as templates for transcription. Probes for *in situ* hybridization were synthesized using MAXIscript Sp6 or T7 (Ambion) in the presence of the DIG RNA labeling mix (Roche). Probes for Northern blots were synthesized with MAXIscript Sp6 or T7 in the presence of 1.85 MBq of [α-^{32}P] UTP (Amersham Biosciences). For detection of plus-strand HCV RNA, minus-strand RNA probes were generated using pcDNA3-TME2 (*Hin*dIII for linearization), pcDNA3-NS3 (*Hin*dIII), and pcDNA3-NS5B (*Bam*HI) as templates for *in vitro* transcription. For detection of minus-strand HCV RNA, plus-strand RNA probes were generated using pcDNA3-TME2 (*Eco*RI), pcDNA3-NS3 (*Xba*I), and pcDNA3-NS5B (*Bam*HI) as templates. The RNA probes used for *in situ* hybridization were subjected to alkaline hydrolysis to generate fragments of ~170 nucleotides in length. Synthesized RNA probes were treated with DNase I (Ambion) and size fractionated using MicroSpin G-50 columns (Amersham Biosciences).

Sucrose density gradient centrifugation of culture medium

The 100-time concentrated medium from JFH1-bearing cells was loaded onto 20-50% [w/v] sucrose gradient containing 50 mM Hepes-KOH (pH 7.4), 100 mM NaCl and 1mM EDTA followed by centrifugation at 100,000 x g for 16 hrs using RPS40T rotor of HITACHI ultracentrifuge. The gradient was fractionated into 31 fractions. Buoyant density of each fraction was analyzed by Abe refractometer (ATAGO Inc., Japan). Each fraction was dialyzed against serum free DMEM and was used for the infection experiment as well as quantification of Core and HCV RNA titer as described above.

Infection experiments

Cells were cultured in DMEM containing 5% FBS. The medium was collected and mixed with a 0.01 volume of 1 M HEPES (pH 7.4). After filtering the sample through a 0.22-μm filter (Millipore), the filtrate was concentrated by reducing the volume to

between 1/50 and 1/100 of the original volume with an Amicon Ultra-15 centrifugal filter with Ultracel-100 membrane (Millipore). Huh-7.5 cells seeded on a collagen-coated Labtech II 8-well chamber were incubated with 100 μl of the concentrated medium for 120 min. Then, the cells were washed three times with DMEM. Twenty-four hours after the inoculation, the cells were labeled with serum from HCV-infected patients to determine the infectivity level.

***In situ* hybridization analysis**

Huh-7 cells transfected with JFH1 RNA were seeded on a collagen-coated Labtech II 8-well chamber (Nunc). Three days after seeding, the cells were washed twice with PBS and fixed with fixation solution for 15 min at room temperature. Then, the cells were permeabilized with 0.05% Triton X-100 in fixation solution for 15 min at room temperature. After washing the cells twice with cold DEPC-treated PBS, the cells were incubated in 95% formamide and 0.1x SSC (1x SSC: 150 mM NaCl and 15 mM sodium citrate) for 15 min at 65°C. After chilling the chamber on ice, the cells were incubated in 100 μl of pre-hybridization solution for 60 min at room temperature. Pre-hybridization solution was composed of 50% formamide, 2x SSC, 1 μg/ml of salmon sperm DNA (sonicated to 1-2 kb pieces, Roche), 1 μg/ml of yeast tRNA (Roche), and 2 mM vanadyl ribonucleoside complex (NEB). Then, the cells were incubated in 100 μl of hybridization solution (pre-hybridization solution containing 10% dextran sulfate and 100 to 500 ng/ml of the RNA probes) for 40 hrs at 42°C. After the hybridization, the slide glass in the chamber was transferred to a bucket filled with wash solution 1 (50% formamide and 2x SSC at pH 7.4) and washed three times for 20 min at 50°C with gentle agitation. Then, the slide was washed three more times in wash solution 2 (0.1x SSC at pH 7.4) for 20 min at 50°C with gentle agitation. The slide was incubated in blocking solution for 30 min at room temperature. To detect DIG-labeled probes, sheep anti-DIG antibodies (Roche) and Alexa 488 or Alexa 568 anti-sheep IgG antibodies (Invitrogen) were used as primary and secondary antibodies, respectively. When HCV RNA, Core, and NS5A were simultaneously labeled in the same sample, anti-DIG antibodies and the Alexa-conjugated antibodies were incubated with the samples separately to avoid cross-reaction of the Alexa 488 or Alexa 568 anti-sheep IgG antibodies with mouse and rabbit IgG. Briefly, the incubation with the anti-DIG antibodies and the Alexa 488 anti-sheep IgG antibodies was performed first. After

washing with PBS followed by a second fixation procedure, the cells were incubated with anti-Core and anti-NS5A antibodies followed by Alexa 568 anti-rabbit IgG and Alexa 647 anti-mouse IgG antibodies. For treatment with nuclease, digitonin-permeabilized cells were treated with 1 μg/ml of RNase A in the presence or absence of 0.05% Triton X-100 for 15 min at 37°C. After the treatment, RNase A was inactivated by incubation with 4% formaldehyde. Then, the cells were completely permeabilized with 0.05% Triton X-100 for 5 min at room temperature.

Statistical analysis of the recruitment of viral components to the LD

Only the cells that have any LDs surrounded by HCV proteins, PDI, or HCV RNA were counted as positive under immunofluorescence microscopy, and those adjacent to HCV signal were not included. The obtained cell number was divided by the total number of HCV replicating cells and is shown as "% cells with HCV protein-LD colocalization". In case of the chimeras Con1/C3 and H77/C3 LD colocalization with HCV proteins was additionally analyzed by using the ImageJ RG2B software package (Rasband, W.S., ImageJ, U. S. National Institutes of Health, Bethesda, Maryland, USA, http://rsb.info.nih.gov/ij/, 1997-2006.). Approximately 200 cells were examined for each antigen.

RNA-protein binding precipitation assay

In vitro translated [^{35}S]-labeled products (Core^{Wt} and Core$^{PP/AA}$) were incubated with poly-U or protein G Sepharose resin in 50 mM HEPES (pH7.4), 100 mM NaCl, 0.1 % NP-40, and RNase inhibitor at 4°C for 2 hrs. After five washes, resin-bound radiolabeled proteins were analyzed by gel electrophoresis followed by autoradiography.

Supplementary References

1. Blight, K. J., McKeating, J. A. & Rice, C. M. Highly permissive cell lines for subgenomic and genomic hepatitis C virus RNA replication. *J Virol* **76**, 13001-14 (2002).
2. Lohmann, V. et al. Replication of subgenomic hepatitis C virus RNAs in a hepatoma cell line. *Science* **285**, 110-3 (1999).
3. Miyanari, Y. et al. Hepatitis C virus non-structural proteins in the probable membranous compartment function in viral genome replication. *J Biol Chem* **278**, 50301-8 (2003).
4. Takeuchi, T. et al. Real-time detection system for quantification of hepatitis C virus genome. *Gastroenterology* **116**, 636-42 (1999).
5. Tauchi-Sato, K., Ozeki, S., Houjou, T., Taguchi, R. & Fujimoto, T. The surface of lipid droplets is a phospholipid monolayer with a unique Fatty Acid composition. *J Biol Chem* **277**, 44507-12 (2002).
6. Pietschmann, T. et al. Construction and characterization of infectious intragenotypic and intergenotypic hepatitis C virus chimeras. *Proc Natl Acad Sci U S A* **103**, 7408-13 (2006).

THE JOURNAL OF BIOLOGICAL CHEMISTRY VOL. 282, NO. 45, pp. 32765–32772, November 9, 2007

Anti-hepatitis C Virus Activity of Tamoxifen Reveals the Functional Association of Estrogen Receptor with Viral RNA Polymerase NS5B*

Received for publication, May 30, 2007, and in revised form, August 15, 2007 Published, JBC Papers in Press, August 17, 2007, DOI 10.1074/jbc.M704418200

Koichi Watashi, Daisuke Inoue, Makoto Hijikata, Kaku Goto, Hussein H. Aly, and Kunitada Shimotohno[1]

From the Department of Viral Oncology, Institute for Virus Research, Kyoto University, 53 Kawaharacho, Shogoin, Sakyo-ku, Kyoto 606-8507, Japan

Hepatitis C virus (HCV) is a major causative agent of hepatocellular carcinoma. HCV genome replication occurs in the replication complex (RC) around the endoplasmic reticulum membrane. However, the mechanisms regulating the HCV RC remain widely unknown. Here, we used a chemical biology approach to show that estrogen receptor (ESR) is functionally associated with HCV replication. We found that tamoxifen suppressed HCV genome replication. Part of ESRα resided on the endoplasmic reticulum membranes and interacted with HCV RNA polymerase NS5B. RNA interference-mediated knockdown of endogenous ESRα reduced HCV replication. Mechanistic analysis suggested that ESRα promoted NS5B association with the RC and that tamoxifen abrogated NS5B-RC association. Thus, ESRα regulated the presence of NS5B in the RC and stimulated HCV replication. Moreover, the ability of ESRα to regulate NS5B was suggested to serve as a potential novel target for anti-HCV therapeutics.

Estrogen receptor (ESR)[2] belongs to the steroid hormone receptor family of the nuclear receptor superfamily (1). ESR consists of two subtypes, ESRα and ESRβ. As a primary physiological function, ESR is involved in the transcription for downstream genes in response to stimulation by the ligand, estradiol. In the normal state, ESR is mainly located in the cytoplasm and nucleus. Upon binding of the ligand, ESR dimerizes and translocates into the nucleus, where it binds to the ESR-responsive elements (ERE) in the DNA promoter of downstream genes and drives transcription. In addition to this classical genomic action, a portion of ESR is located on the membrane, such as the plasma membrane, and involved in the nongenomic function of triggering signal transduction pathways, such as mitogen-activated protein kinase, phosphatidylinositol 3-kinase, and protein kinase C (2–4). Although the molecular basis of ESR membrane retention is not fully understood, one mechanism involves a membrane protein, caveolin (CAV); ESRα interacted with CAV, and this interaction facilitated ESRα localization to the membrane (5, 6). It was also reported that ESRα localizes to the lipid rafts on the plasma membrane (7). The lipid rafts are microdomains of the membrane that form platforms enriched in cholesterol and glycosphingolipids. However, the characteristics and relevance of membrane-associated ESR have not been fully disclosed. Here, we report the novel role of ESRα in the regulation of viral replication.

Hepatitis C virus (HCV), a causative agent of chronic hepatitis, liver cirrhosis, and hepatocellular carcinoma, constitutes a serious health problem worldwide (8). HCV has a positive strand RNA genome that produces at least 10 functional viral proteins: core, envelope 1, envelope 2, p7, nonstructural protein 2 (NS2), NS3, NS4A, NS4B, NS5A, and NS5B (9, 10). NS5B is an RNA-dependent RNA polymerase, which plays a central role in viral genome replication (11, 12). HCV genome replication can be evaluated using a HCV subgenomic replicon system, which Lohmann *et al.* (13) first established. In this system, cells carry an HCV subgenome RNA encoding NS3 to NS5B. Using this system, it has been proposed that HCV genome replication occurs in the replication complex (RC), which contains the viral genome RNA and HCV NS proteins. The RC forms on the surface of the intracellular membranes, including the endoplasmic reticulum (ER) membrane, and is surrounded by a membrane structure (14–17). It also has been reported that HCV genome replication associates with the lipid rafts on these intracellular membranes, such as the ER membrane (14, 18). These lipid rafts accumulate CAV2, and HCV proteins involved in viral genome replication cofractionate with CAV2 (18). However, it is largely unknown how the RC is formed and under what mechanism the HCV proteins participate in the RC.

A chemical biology approach is a useful method to analyze the molecular mechanism of viral life cycles as well as cellular physiological processes (19). We employed forward chemical genetics in which we analyzed HCV replication activity as a phenotypic indicator of a cell-based assay to screen chemical

* This work was supported by grants-in-aid for cancer research and for the second term comprehensive 10-year strategies for cancer control from the Ministry of Health, Labor, and Welfare; by grants-in-aid for scientific research from the Ministry of Education, Culture, Sports, Science, and Technology; by grants-in-aid for the Research for the Future Program from the Japanese Society for the Promotion of Science; and by grants-in-aid for the Program for Promotion of Fundamental Studies in Health Science from the Organization for Pharmaceutical Safety. The costs of publication of this article were defrayed in part by the payment of page charges. This article must therefore be hereby marked "*advertisement*" in accordance with 18 U.S.C. Section 1734 solely to indicate this fact.

[1] To whom correspondence should be addressed: Dept. of Viral Oncology, Institute for Virus Research, Kyoto University, 53 Kawaharacho, Shogoin, Sakyo-ku, Kyoto 606-8507, Japan. Tel.: 81-75-751-4000; Fax: 81-75-751-3998; E-mail: kshimoto@virus.kyoto-u.ac.jp.

[2] The abbreviations used are: ESR, estrogen receptor; HCV, hepatitis C virus; RC, replication complex; ER, endoplasmic reticulum; TAM, tamoxifen; ERE, ESR-responsive element(s); CAV, caveolin; NS, nonstructural protein; MM, microsomal membrane; siRNA, small interfering RNA; si-ESR, small interfering ESR; GST, glutathione *S*-transferase; aa, amino acid(s); RT, reverse transcription; NS3, NS4A, NS4B, NS5A, and NS5B, nonstructural protein 3, 4A, 4B, 5A, and 5B, respectively.

compounds that inhibited HCV replication. Using this system, we previously identified an immunosuppressant, cyclosporin A, as an anti-HCV compound (20). We also reported that cyclophilin B regulated the RNA binding activity of NS5B (21). In the current study, this chemical screening approach linked ESRα to HCV replication. We showed that tamoxifen (TAM) suppressed HCV genome replication. Using TAM as a bioprobe, we found that ESRα interacted with NS5B and regulated the participation of NS5B in the RC.

EXPERIMENTAL PROCEDURES

Cell Culture and Transfection—Huh-7 and cured MH-14 cells (21) were cultured in Dulbecco's modified Eagle's medium (Invitrogen) supplemented with 10% fetal bovine serum, minimal essential medium nonessential amino acid (Invitrogen), and kanamycin (Meiji). MH-14 cells, carrying HCV subgenomic replicon (16), and LucNeo#2 cells, carrying luciferase-containing subgenomic replicon (22), were cultured in the same medium supplemented with 300 μg/ml G418 (Invitrogen). Hus-E7/DN24 cells, a human hepatocyte cell line established by immortalization with HPV E6E7 and hTERT from human primary hepatocytes and introduction with a dominant negative form of interferon regulatory factor-7 (23), were cultured with Dulbecco's modified Eagle's medium with 20 mM Hepes (Invitrogen), 15 g/ml L-proline, 0.25 g/ml insulin (Sigma), 50 nM dexamethasone (Sigma), 44 mM $NaHCO_3$, 10 mM nicotinamide, 5 ng/ml epidermal growth factor, 0.1 mM Asc-2P, 100 IU/ml penicillin G (Invitrogen), 100 μg/ml streptomycin (Invitrogen), 5% fetal bovine serum, 1% Dulbecco's modified Eagle's medium, and 2 UG/ml Fungizone (Invitrogen) (24). Plasmid transfection was performed with FuGENE 6 transfection reagent (Roche Applied Science), as described previously (25). RNA transfection was achieved using DMrie-C transfection reagent (Invitrogen), as described previously (21). siRNA was transfected by using siLentFect (Bio-Rad) (21).

Plasmid Construction—pCMV-FL-ESRα, encoding the whole open reading frame of ESRα fused with a FLAG tag, was generated by inserting the PCR product using 5′-GTTGAATTCATGACCATGACCCTCCAC-3′ and 5′-GTTGATCTCGAGTCAGACTGTGGCAGGGAAAC-3′ as primer set and human lymphocyte cDNA library (Clontech) as a template into the EcoRI-XhoI site of pCMV-FLAG vector (21). pCAG-HA-NS5B, encoding the NS5B protein fused with a hemagglutinin tag, was made by subcloning the PCR product with 5′-GTTGCGGCCGCTATGTCAATGTCCTACTCA-3′ and 5′-GTTCTCGAGTCACCGGTTGGGGAGCAGGTA-3′ as primers and pMH14 as a template into NotI-XhoI digestion of PCAG-HA vector (21). Expression plasmids for HCV NS3, NS4B, NS5A, and NS5B (pcDNA-NS3, pcDNA-NS4B, pcDNA-NS5A, and pcDNA-NS5B, respectively) were described in Ref. 21. pGEX-ESRα A/B, C, D, and E/F, expressing the fusion protein of the domain A/B, C, D, and E/F of ESRα with GST, were prepared by the insertion of the PCR product with pCMV-FL-ESRα as a template and appropriate primers into the EcoRI-XhoI site of pGEX-6P1 vector (Clontech). The expression plasmids for the point mutants of ESRα, ESRα(L540Q), ESRα(255M), and ESRα(258M), of which Leu at aa 540, IRK at aa 255–257, and DRR at aa 258–260 were replaced by Gln, TGT, and ANT, respectively, was generated by oligonucleotide-directed mutagenesis. pCMV-FL-CAV2, encoding FLAG-tagged CAV2, was prepared by inserting the PCR product amplified with 5′-GTTGTCGACTATGGGGCTGGAGAC-3′ and 5′-GTTAAGCTTTCAATCCTGGCTC-3′ as primers and human liver cDNA library (Clontech) as a template into the SalI-HindIII site of pCMV-FLAG vector (21). The mammalian expression vector for the C domain of ESRα was generated by replacing the EcoRI-XhoI digestion of pCMV-FLAG vector (21) by that of pGEX-ESRα C. pLMH14 was described previously (26). pGL3-EREX3-TATA-Luc, pcDNA3-ERα, pcDNA3-hERβ were kindly provided by Dr. Kato (Institute of Molecular and Cellular Biosciences, University of Tokyo). JFH1 expression plasmid was provided by Dr. Wakita (National Institute of Infectious Diseases).

Luciferase Assay—A luciferase assay monitoring HCV replication activity was performed as described previously (22, 26). In Fig. 1, *A* and *F*, we used LucNeo#2 cells, stably carrying luciferase-containing subgenomic replicon (22). In Figs. 2 (*D* and *E*), 4*C*, and 6*A*, we transiently transduced luciferase-containing replicon LMH14 RNA together with each expression plasmid into cured MH-14 cells (26). A luciferase assay detecting the transcriptional activity driven from the ERE was performed as described previously (25).

Real Time RT-PCR Analysis—Real time RT-PCR analysis was performed as previously described (20).

Immunoblot Analysis—Immunoblot analysis was performed as previously described (25). The antibodies used in this study are anti-NS5A (kindly provided by Dr. Takamizawa (Osaka University)), anti-NS5B (anti-NS5B#14; a generous gift from Dr. Kohara (Tokyo Metropolitan Institute of Medical Science)), anti-NS5B (NS5B#6; a kind gift from Dr. Fukuya (Osaka University)), anti-tubulin (Oncogene), anti-FLAG (Sigma), anti-IκBα (Santa Cruz Biotechnology, Inc., Santa Cruz, CA), anti-calnexin (StressGen), and anti-caveolin-2 antibodies (BD Biosciences Pharmingen).

Indirect Immunofluorescence Analysis—Indirect immunofluorescence analysis was performed as described previously (25). The antibodies used were anti-NS5A and anti-protein-disulfide isomerase antibodies (StressGen).

siRNA—siRNA duplexes (5′-GUGUGCAAUGACUAUGCUUCA-3′ for si-ESRα and 5′-CGCAUCGGGAUAUCACUAUGG-3′ for si-ESRβ) were synthesized (Proligo). A randomized siRNA, si-control, was purchased from Dharmacon (nonspecific control duplex IX).

Enzyme-linked Immunosorbent Assay—HCV core was quantified in the culture medium of the cells transfected with JFH1 RNA (29) with an enzyme-linked immunosorbent assay according to the manufacturer's protocol (HCV antigen enzyme-linked immunosorbent assay test; Ortho-Clinical Diagnostics).

RT-PCR Analysis—RT-PCR analysis was performed as described (20) by using the following primer sets: 5′-CCTACTACCTGGAGAACG-3′ and 5′-GCTGGACACATATAGTCG-3′ for the detection of ESRα and 5′-AGCCATGACATTCTATAGC-3′ and 5′-CCACTTCGTAACACTTCC-3′ for ESRβ.

GST Pull-down Assay—The GST pull-down assay was conducted as described previously (25).

Immunoprecipitation Analysis—Immunoprecipitation analysis was performed as described previously (25). The antibodies

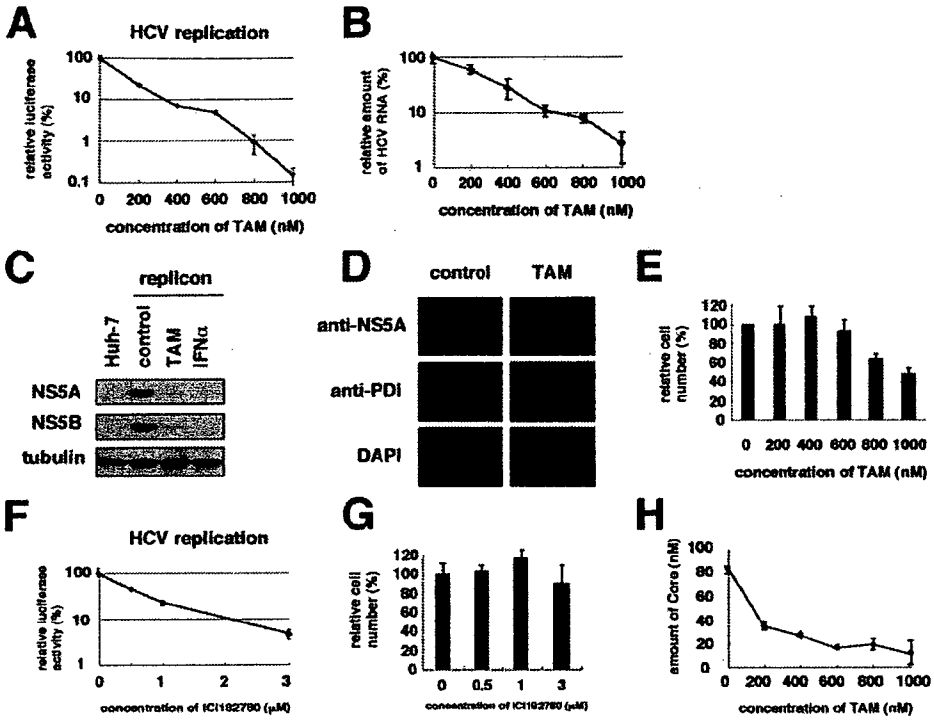

FIGURE 1. **TAM suppressed the replication of the HCV genome.** *A*, luciferase activities were measured using the LucNeo#2 cells, which carried a luciferase-containing replicon RNA, upon treatment with TAM at the indicated doses for 7 days. Relative luciferase activities are plotted against the concentrations of TAM. The data show the means of three independent experiments. The *error bars* are indicated. *B*, HCV RNA was quantified by real time RT-PCR analysis using the lysates from MH-14 cells, harboring the HCV subgenomic replicon, treated with the indicated doses of TAM for 7 days. Relative amounts of HCV RNA are shown. *C*, HCV NS5A and NS5B proteins as well as tubulin as an internal control were detected by immunoblot analysis in the lysates from MH-14 cells (replicon) treated without (control) or with 500 nM TAM or 100 IU/ml interferon-α as a positive control for 7 days and Huh-7 cells. *D*, HCV NS5A and protein-disulfide isomerase (*PDI*) as an internal control were detected by indirect immunofluorescence analysis in the cells treated without (control) or with 500 nM TAM for 7 days. 4′,6-Diamidino-2-phenylindole (*DAPI*) shows a nuclear staining. *E*, cell number was counted after 5 days upon treatment with various concentrations of TAM. Relative cell numbers are shown. *F*, luciferase activities with LucNeo#2 cells treated with various concentrations of ICI182780 were measured as described in *A*. *G*, cell number was counted under treatment with ICI182780 at the indicated concentrations. *H*, core in the culture medium of JFH1 RNA-transfected cells upon treatment with TAM was quantified as described under "Experimental Procedures."

used in this study were mouse normal IgG as a negative control (Zymed Laboratories), anti-NS5B (anti-NS5B#10; a generous gift from Dr. Kohara at the Tokyo Metropolitan Institute of Medical Science), anti-FLAG, and anti-caveolin-2 antibodies.

Fractionation of Cell Extracts—MH-14 cells transfected with the expression plasmid for FLAG-tagged ESRα were fractionated essentially as described previously (25).

HCV Replication Complex Assay—Isolation of HCV RC was done as described previously (16, 21).

In Vitro HCV Infection Experiment—*In vitro* HCV infection was conducted essentially as described (23). Briefly, HCV-infected serum (~2×10^5 copies) was inoculated into HuS-E7/DN24 cells (5×10^4 cells) for 24 h. After washes, cells were cultured in the medium supplemented with 10 μM PD98059 to stimulate HCV translation (27) (*scheme* in Fig. 6*B*). To observe HCV amplification, HCV RNA in the cells was quantified, since HCV RNA was hardly detected significantly in the culture medium (23).

3-(4,5-Dimethylthiazol-2-yl)-2,5-diphenyltetrazolium bromide Assay—The 3-(4,5-dimethylthiazol-2-yl)-2,5-diphenyltetrazolium bromide assay was performed to examine the cell viability using Cell Proliferation kit II, XTT (Roche Applied Science) according to the manufacturer's protocol.

RESULTS

Tamoxifen Suppressed HCV Genome Replication—We screened for agents that suppressed HCV genome replication using a HCV subgenomic replicon system (13, 16). Among the compounds tested, we observed that TAM inhibited HCV genome replication. HCV replication activity, monitored by luciferase activity (22), and the amount of HCV RNA were decreased with TAM treatment in a dose-dependent manner (Fig. 1, *A* and *B*). The expression of HCV proteins, NS5A and NS5B, detected by immunoblot (Fig. 1*C*) and indirect immuofluorescence analyses (Fig. 1*D*), also drastically decreased by treatment with TAM. A high concentration of TAM decreased cell proliferation (Fig. 1*E*). However, TAM suppressed HCV replication without any cytotoxicity in another cell line, HuS-E7/DN24 cells (Fig. 6, *C* and *D*). In addition, a pure anti-estrogen compound ICI182780, which had little cytotoxic effect, reduced HCV RNA (Fig. 1, *F* and *G*). Moreover, TAM inhibited the production of core in the culture medium of HCV JFH1-transfected cells, in a recently developed system of the production of infectious HCV particles (Fig. 1*H*) (28–30). The above data indicate that TAM suppresses HCV genome replication.

ESR Was Involved in HCV Genome Replication—Next, we investigated which cellular protein TAM targets to suppress HCV replication. It has been reported that TAM targets 1) ESR (31), 2) P-glycoprotein (32, 33), 3) calmodulin (34), 4) protein kinase C (35, 36), etc. Although other compounds targeting P-glycoprotein, calmodulin, and protein kinase C did not affect HCV replication in our screening (data not shown), ESR was suggested to play a role in HCV replication as shown below.

RNAi-mediated specific knockdown of endogenous ESRα and ESRβ (Fig. 2*A*) reduced HCV RNA in replicon-containing cells to ~20–40% and 60–70%, respectively (Fig. 2*B*). Transient transfection with ESRα and ESRβ expression plasmids, which activated ERE-driven transcription 4–5-fold (Fig. 2*C*), showed that ectopically expressed ESRα augmented HCV replication activity in a dose-dependent manner, whereas ESRβ did not (Fig. 2*D*). ESRα-induced augmentation of the replication was reversed upon TAM treatment (Fig. 2*D*). These results suggested a significant role of ESR, especially ESRα, in HCV

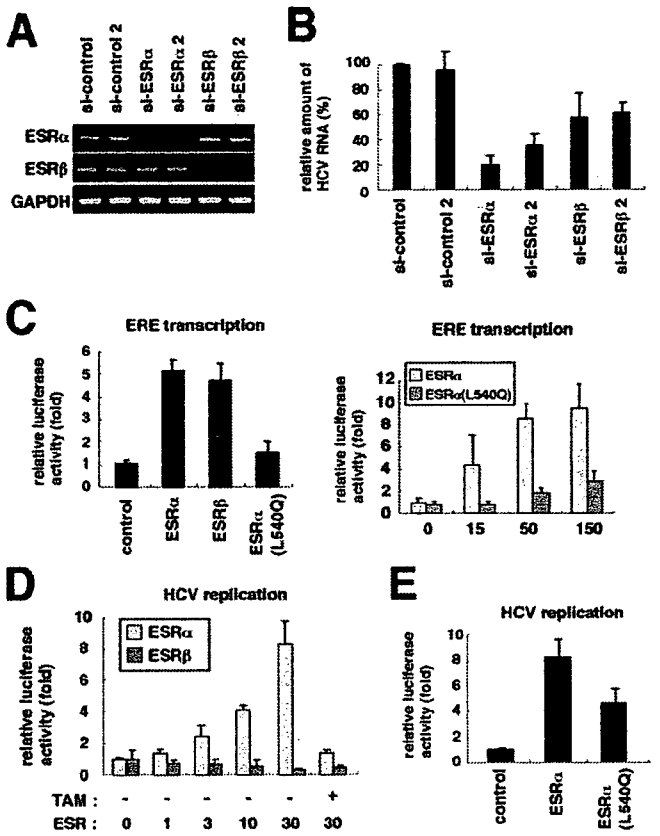

FIGURE 2. **ESR was involved in HCV genome replication.** *A*, specific knockdown of endogenous ESRα and ESRβ. RT-PCR analysis was performed to detect the expression of ESRα, ESRβ, and glyceraldehyde-3-phosphate dehydrogenase (*GAPDH*) as an internal control in the cells transfected with siRNA recognizing ESRα (si-ESRα, si-ESRα2), ESRβ (si-ESRβ, si-ESRβ2), or randomized siRNA (si-control, si-control2). *B*, HCV RNA was quantified as shown in Fig. 1*B*, using the cells transfected with si-control, si-control2, si-ESRα, si-ESRα2, si-ESRβ, and si-ESRβ2 for 5 days. *C*, the ERE-mediated transcriptional activities were measured by a luciferase assay using the lysates from the cells transfected with pGL3-EREX3-TATA-Luc reporter plasmid together with pcDNA3-ERα (ESRα), pcDNA3-hERβ (ESRβ), pcDNA-ESRα(L540Q), or the empty vector (control) (*left*) or varying amounts (ng) of pcDNA3-ERα (ESRα) or pcDNA-ESRα(L540Q) (*right*) and treated with 100 nM estradiol for 36 h. *D* and *E*, HCV replication activities were examined by quantifying the luciferase activities using cured MH-14 cells transfected with the indicated doses (ng) of ESRα or ESRβ (*D*) or 30 ng of ESRα, ERα(L540Q), or the empty vector (control) (*E*) together with 0.125 μg of LMH14 RNA without or with 1 μM TAM for 4 days.

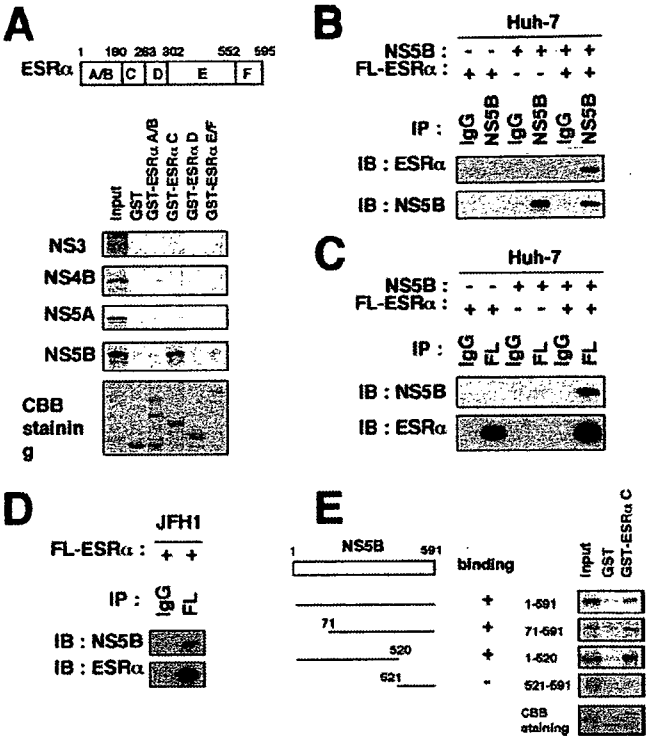

FIGURE 3. **ESRα interacted with HCV NS5B.** *A*, *top*, schematic representation of the primary structure of ESRα. ESRα consists of domains A–F. The amino acid numbers are also shown. *Bottom*, GST pull-down assays were performed using the recombinant proteins of the A/B, C, D, and E/F domain of ESRα fused with GST and *in vitro* translated HCV NS3, NS4B, NS5A, and NS5B protein. *Input*, the one-fifth amount of protein used for the pull-down assay. The Coomassie Brilliant Blue staining pattern of the precipitated fraction is also shown in the *bottom panel*. *B–D*, the lysates from the cells ectopically expressing NS5B (*B* and *C*) or the whole open reading frame of the HCV JFH1 strain (*D*) and/or FLAG-tagged ESRα were immunoprecipitated (*IP*) with anti-NS5B (*B*; NS5B), anti-FLAG antibody (*C* and *D*; FL), or mouse normal IgG as a negative control followed by the detection of ESRα and NS5B by immunoblot analysis (*IB*). *E*, deletion mutants of NS5B were subjected to a GST pull-down assay with GST-fused C domain of ESRα as described in *A*. The *left panel* shows a schematic representation of the full-length and truncated mutants of NS5B. The *numbers* indicate the amino acid numbers in NS5B.

genome replication. ESRα(L540Q), carrying a leucine to glutamine point mutation at aa 540 within the L*XX*LL motif (aa 536–540) of ESRα (37), had much lower transactivation activity driven from ERE (Fig. 2*C*). However, ESRα(L540Q) stimulated HCV replication activity ~5-fold, although the stimulation was less than that by wild-type ESRα (Fig. 2*E*). Thus, ESRα having lower transactivating capacity could still facilitate HCV replication.

ESRα Interacted with HCV NS5B—Thus, the chemical biology approach revealed the involvement of ESR in HCV genome replication. Then we investigated the molecular mechanism of ESR-induced HCV replication. A binding assay between ESRα and HCV proteins expressed in the HCV subgenomic replicon showed that the C domain of ESRα coprecipitated with NS5B but not NS3, NS4B, and NS5A (Fig. 3*A*). Other ESRα domains, A/B, D, and E/F, did not bind to any HCV proteins. A coimmunoprecipitation assay also indicated the presence of ESRα in the immunoprecipitate by anti-NS5B antibody (Fig. 3, *B* and *D*), and *vice versa* (Fig. 3*C*). Thus, ESRα specifically interacted with NS5B. Deletion analysis indicated that the region of 71–591 and 1–520 but not 521–591 of NS5B coprecipitated with the recombinant C domain of ESRα (Fig. 3*E*). This binding profile is different from that between cyclophilin B and NS5B, which we previously reported (21).

The ESRα-NS5B Interaction Was Important for the Regulation of HCV Genome Replication—To examine whether the interaction between ESRα and NS5B was essential for the ESRα-mediated regulation of HCV replication or not, we searched for a point mutant of ESRα that could not bind to NS5B by alanine-scanning mutation analysis. ESRα mutants, ESRα(255M) and ESRα(258M), in which IRK at aa 255–257 and DRR at aa 258–260 was replaced by TGT and AQT, respectively, had little affinity with NS5B (Fig. 4*A*) but still possessed the ERE-mediated transactivation capacity (Fig. 4*B*). However, both ESRα(255M) and ESRα(258M) caused only weak activations of HCV replication, compared with wild type ESRα (Fig. 4*C*). The data suggest that the interaction of ESRα with NS5B is

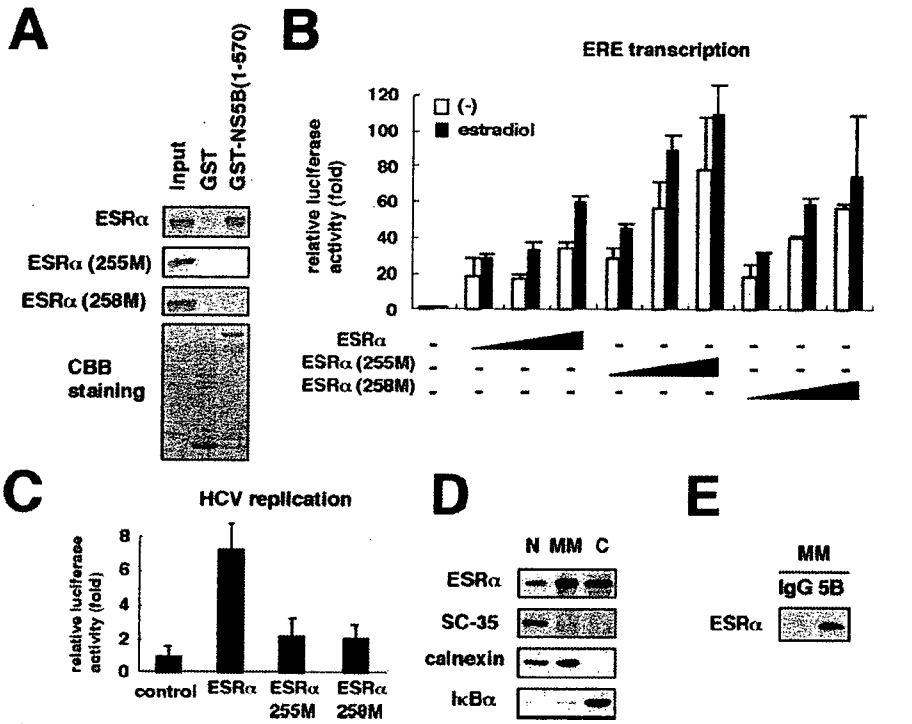

FIGURE 4. **The interaction of NS5B mediated the regulation of HCV genome replication by ESRα.** *A*, GST pull-down assays were performed as described in Fig. 3*A* using the wild type ESRα or point mutant of ESRα, ESRα(255M), and ESRα(258M). *B*, the mutation within ESRα(255M) and ESRα(258M) did not reduce the activation capacity of ERE-mediated transcription. Huh-7 cells were transfected with the expression plasmids for ESRα, ESRα(255M), or ESRα(258M) at doses of 10, 30, and 100 ng each together with pGL3-EREX3-TATA-Luc reporter plasmid and treated without (*white bar*) or with 100 nM estradiol (*black bar*) to quantify the luciferase activity. *C*, HCV replication activities were examined by quantifying the luciferase activities as described in the legend to Fig. 2*D* in the cells upon transfection with the expression plasmids for wild type ESRα, ESRα(255M), or ESRα(258M). *D*, the cells were fractionated into the nucleus (*N*), MM, and cytoplasm (*C*). Each fraction was detected for FLAG-tagged ESRα, SC-35, calnexin, and IκBα, respectively, by immunoblot analysis. Calnexin, an ER marker protein, was detected in the nucleus as well as MM, probably because of the existence of the nuclear membrane in the nuclear fraction. *E*, the MM fraction obtained in *D* was subjected to a coimmunoprecipitation assay using anti-NS5B or IgG followed by immunoblot analysis for the detection for ESRα.

critical for ESRα-mediated regulation of HCV genome replication.

Thus, ESRα interaction with NS5B regulates HCV replication. NS5B is mainly located on the cytoplasmic surface of the ER membrane (21, 38). On the other hand, ESRα as a nuclear hormone receptor is normally distributed in the cytoplasm and translocates into the nucleus upon ligand stimulation. In addition, a part of ESRα localizes on the membrane fraction. In our experiment, NS5B was mainly located around the ER, colocalized with the ER marker, protein-disulfide isomerase (data not shown) (21). Ectopically expressed ESRα showed diffuse distribution in the cells (data not shown). We fractionated cell homogenates and observed that a part of the ESRα resided in the microsomal membrane (MM) fraction (Fig. 4*D*). Moreover, ESRα in the MM fraction was coprecipitated with NS5B (Fig. 4*E*). It suggests the possibility that the interaction between NS5B and ESRα, at least in part of them, occurs on the ER membrane.

ESRα Promoted the Participation of NS5B in the HCV Replication Complex—It was reported that HCV proteins involved in the replication machinery was associated with the lipid raft on the ER and cofractionated with CAV2. A coimmunoprecipitation assay showed that NS5B associated with CAV2 (Fig. 5*A*). In the experiment investigating the role of ESRα in NS5B-CAV2 association, the coprecipitation of NS5B with CAV2 was decreased upon the knocking down of ESRα (Fig. 5*B*). Treatment with TAM abrogated the association of NS5B with CAV2 (Fig. 5*C*), although the total amount of NS5B in the cells is similar in the presence and absence of TAM for 24 h in this experiment (data not shown). Thus, ESRα was suggested to promote the association between NS5B and CAV2. Since a part of CAV2 resided on the lipid raft on the ER (18), ESRα-mediated binding between NS5B and CAV2 was possible to affect the localization of NS5B to the HCV RC. To see the consequential relevance of ESRα on NS5B function, we analyzed the HCV RC by treatment with digitonin/protease as described previously (16). HCV proteins involved in the RC and surrounded by the membrane structure are resistant to the treatment with digitonin followed by protease, whereas those unrelated to the replication outside the RC are digested by the treatment. By using this technique measuring the sensitivity to protease, HCV RC can be distinguished from the ER that is not related to the replication, although the RC and the nucleus cannot be separated. The experimental condition for fractionation was confirmed with the detection with IκBα and calnexin; a cytosolic protein IκBα was washed out following the treatment with digotinin (Fig. 5*D*, *lanes 1* and *2*), and ER protein calnexin, which did not accumulate in the RC, was digested by treatment with digotinin/protease (Fig. 5*D*, *lanes 2–4*). An ER lipid raft component, CAV2, was still detected under the digitonin/protease treatment (the RC-containing fraction) (Fig. 5*D*, *lanes 3* and *4*). Under this condition, a part of NS5B was detected in the digitonin/protease-resistant fraction, as described previously (16) (Fig. 5*D*, *lanes 3* and *4*). However, NS5B in this fraction was decreased upon treatment with TAM (Fig. 5*D*, *lanes 3*, *4*, *7*, and *8*). On the other hand, the amount of NS5A was not significantly changed by TAM treatment. Knocking down of ESRα also disrupted the association of NS5B with the RC-containing fraction (Fig. 5*E*). From the above results, it was suggested that ESRα promoted the participation of NS5B in the RC (also see "Discussion").

ESRα Could Serve as a Molecular Target of Anti-HCV Agents—Finally, we assessed the possibility that the association of ESRα with NS5B could serve as a target of anti-HCV agents. By introducing a decoy peptide against ESRα-NS5B interaction, consisting of the C domain of ESRα into replicon-bearing cells,

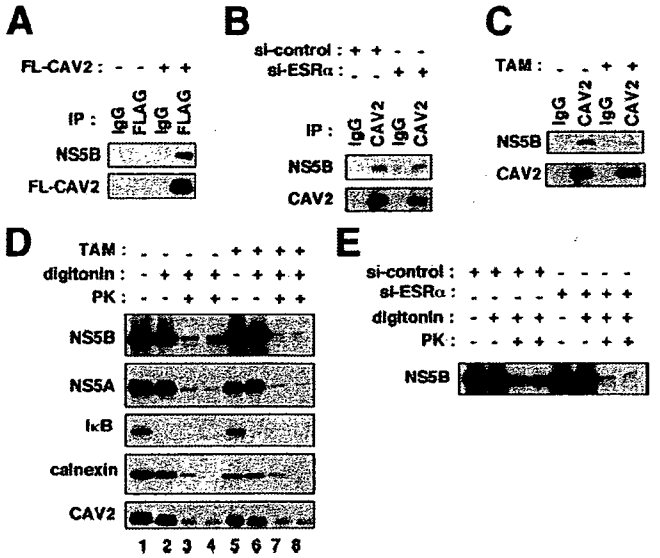

FIGURE 5. **ESRα promoted the participation of NS5B in HCV RC.** *A–C*, a coimmunoprecipitation assay (*IP*) was performed with anti-FLAG (*A*), anti-CAV2 (*B* and *C*) antibody, or mouse normal IgG from the lysates of the cells transfected without or with FLAG-tagged CAV2 (*A*), transfected with si-control or si-ESRα (*B*), or treated without or with 1 μM TAM (*C*). NS5B (*top*) and CAV2 (*bottom*) were detected by immunoblot analysis. *D*, detection of the amount of NS5B in the digitonin/protease-resistant fraction. MH-14 cells were treated without (*lanes 1–4*) or with 1 μM TAM (*lanes 5–8*) for 24 h. Cells were then treated without (*lanes 1* and *5*) or with digitonin (*lanes 2–4* and *6–8*), followed by digestion with proteinase K (0 μg/ml for *lanes 2* and *6*, 0.3 μg/ml for *lanes 3* and *7*, and 1 μg/ml for *lanes 4* and *8*). NS5B, NS5A, IκBα, calnexin, and CAV2 were detected by immunoblot analysis. *E*, HCV RC was isolated as described in *D* using the cells transfected with si-control or si-ESRα, and NS5B was detected. A similar result was obtained by using si-ESRα2.

HCV replication activity was reduced in a dose-dependent manner (Fig. 6*A*). To further observe the significance of ESRα in a physiological condition, we performed an *in vitro* infection experiment using serum from an HCV-infected patient as a nascent virus inoculum and nonneoplastic human hepatocytes as highly infection-permissive cells (Fig. 6*B*). Treatment with 1 μM TAM did not show a cytotoxic effect on these cells in any time course examined (Fig. 6*C*). However, treatment with TAM as well as cyclosporin A as a positive control inhibited the multiplication of viral genome RNA in the cells along with the time course (Fig. 6*D*). Thus, ESRα could serve as a potent molecular target of anti-HCV agents.

DISCUSSION

In general, viruses take advantage of host cell factors for their replication. So far, some factors have been shown to relevantly regulate HCV replication, including hVAP33 (39, 40), FBL2 (41), and cyclophilin B (21). Among these, FBL2 and cyclophilin B were identified by a chemical biological approach; FBL2 from the observation of an anti-HCV activity of lovastatin and an inhibitor of geranylgeranyl transferase (41–43); cyclophilin B from the inhibitory effect of cyclosporin A on HCV replication (20, 21). In this study, we found a suppressive capacity of TAM to HCV genome replication. Through further examination using TAM, we revealed ESRα as a host cell factor regulating HCV replication and suggested its regulation mechanism.

Currently, it is proposed that HCV RC that replicates the HCV genome is formed on the intracellular membrane, including the ER membrane (14–17). It was also reported that HCV genome replication was associated with the lipid raft on the intracellular membrane (18). Most HCV proteins are not related to the RC, whereas only a minor portion of HCV proteins take part in the RC to drive the viral replication (16). It has remained widely unknown, however, how HCV proteins are regulated to participate in the RC. It was reported that hVAP-33 binds to NS5A and NS5B, and this protein is related to the amount of NS5B in the lipid raft (40). hVAP-33 was speculated to recruit NS5B to the lipid raft, although its molecular mechanism has not been analyzed. This study suggested the interaction between ESRα and NS5B in the ER fraction, although we did not show the existence of ESRα in the RC, since the RC and the nucleus cannot be separated in the digitonin/protease treatment experiment. ESRα promoted the interaction of NS5B with CAV2. Previous papers reported that ESRα bound to CAV1 and CAV2 (6). From these observations, ESRα is

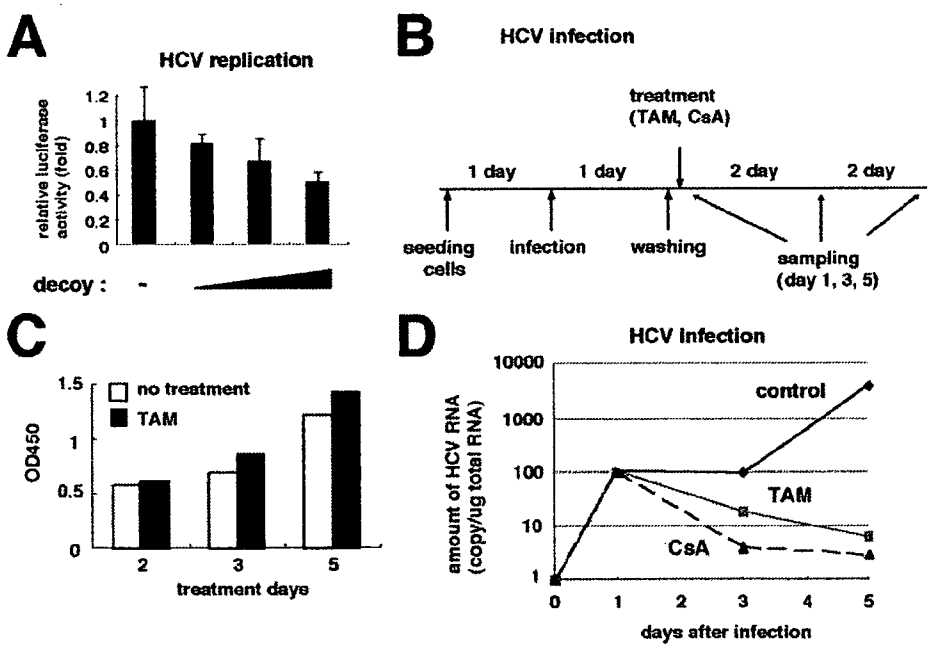

FIGURE 6. **ESRα could serve as a molecular target for anti-HCV agents.** *A*, HCV replication activity was measured by quantifying the luciferase activity as described in the legend to Fig. 2*D* in the cells overexpressing a decoy peptide consisting of the C domain of ESRα. *B*, experimental scheme of *in vitro* HCV infection experiment. After seeding the HuS-E7/DN24 cells, HCV-positive serum was inoculated for 24 h. After extensive washes, the cells were cultured with the medium supplemented without (control) or with 1 μM TAM or 3 μg/ml cyclosporin A. HCV genome RNA was quantified along with the time course (days 1, 3, and 5 postinoculation) by real time RT-PCR analysis. *C*, the treatment with 1 μM TAM did not show any cytotoxic effect on HuS-E7/DN24 cells. 3-(4,5-Dimethylthiazol-2-yl)-2,5-diphenyltetrazolium bromide assays were performed as described under "Experimental Procedures" to examine the viability of the cells at days 2, 3, and 5 postinoculation. *D*, HCV genome RNA was quantified as described in *B* and plotted against the time course.

likely to function as a bridging factor that connects NS5B to CAV2, although we cannot fully neglect the possibility that ESRα augments NS5B-CAV2 binding via another function, such as transcriptional activity. Because CAV2 resided on the lipid raft of the intracellular membrane (18), this action of ESRα may recruit NS5B to the lipid raft and the HCV RC. In fact, ESRα promoted the participation of NS5B in the HCV RC. Thus, ESRα is suggested to escort NS5B to the HCV RC, although it is also possible that ESRα augments the number of the RC itself. However, ESRα at least augments the amount of NS5B involved in HCV replication machinery to stimulate the replication. It was reported that the membrane-associated ESRα served as a platform where signalsomes, including receptor tyrosine kinase, nonreceptor tyrosine kinase Src, and G proteins, assembled and activated downstream signaling pathways (44–46). HCV may also take advantage of such platform characteristics of ESRα to form the RC for their efficient replication. Although the mechanisms of the nuclear receptor function of ESRα have been extensively elucidated, the functions of membrane-associated ESRα have not been widely characterized so far. This study suggested a novel physiological relevance of membrane-associated ESRα as a regulator of the viral replication.

Until now, there are no clinical studies that report a direct interaction of TAM treatment with HCV replication in patients infected with HCV. Given our results, examinations on the effect of TAM or other anti-estrogen drugs may be one of the useful approaches to develop a new anti-HCV strategy. On the other hand, we disclosed the mechanism of ESR-mediated regulation of HCV genome replication. Screening for compounds that inhibit this mechanism expectedly led to novel types of anti-HCV agents. Further analyses on ESR are needed to develop anti-HCV therapeutics as well as reveal the regulation mechanism of HCV replication.

Acknowledgments—We are grateful to Dr. T. Murata, T. Hishiki, and M. Hosaka for establishing the replicon-containing cells. We thank Dr. Aratake (Asahi Kasei Pharma) for helpful discussions. We also thank Dr. Kato, Dr. Takamizawa, Dr. Kohara, Dr. Fukuya, and Dr. Wakita for kindly providing the plasmids: pGL3-EREX3-TATA-Luc, pcDNA3-ERα, and pcDNA3-hERβ; anti-NS5A antibody; anti-NS5B antibody; anti-NS5B antibody; and JFH1 expression plasmid, respectively.

REFERENCES

1. Mangelsdorf, D. J., Thummel, C., Beato, M., Herrlich, P., Schutz, G., Umesono, K., Blumberg, B., Kastner, P., Mark, M., Chambon, P., and Evans, R. M. (1995) *Cell* **83,** 835–839
2. Acconcia, F., and Kumar, R. (2006) *Cancer Lett.* **238,** 1–14
3. Levin, E. R. (2005) *Mol. Endocrinol.* **19,** 1951–1959
4. Song, R. X., Zhang, Z., and Santen, R. J. (2005) *Trends Endocrinol. Metab.* **16,** 347–353
5. Razandi, M., Alton, G., Pedram, A., Ghonshani, S., Webb, P., and Levin, E. R. (2003) *Mol. Cell. Biol.* **23,** 1633–1646
6. Razandi, M., Oh, P., Pedram, A., Schnitzer, J., and Levin, E. R. (2002) *Mol. Endocrinol.* **16,** 100–115
7. Marquez, D. C., Chen, H. W., Curran, E. M., Welshons, W. V., and Pietras, R. J. (2006) *Mol. Cell. Endocrinol.* **246,** 91–100
8. Liang, T. J., Jeffers, L. J., Reddy, K. R., De Medina, M., Parker, I. T., Cheinquer, H., Idrovo, V., Rabassa, A., and Schiff, E. R. (1993) *Hepatology* **18,** 1326–1333
9. Grakoui, A., Wychowski, C., Lin, C., Feinstone, S. M., and Rice, C. M. (1993) *J. Virol.* **67,** 1385–1395
10. Hijikata, M., Kato, N., Ootsuyama, Y., Nakagawa, M., and Shimotohno, K. (1991) *Proc. Natl. Acad. Sci. U. S. A.* **88,** 5547–5551
11. Bartenschlager, R., and Lohmann, V. (2001) *Antiviral Res.* **52,** 1–17
12. Tellinghuisen, T. L., and Rice, C. M. (2002) *Curr. Opin. Microbiol.* **5,** 419–427
13. Lohmann, V., Korner, F., Koch, J., Herian, U., Theilmann, L., and Bartenschlager, R. (1999) *Science* **285,** 110–113
14. Aizaki, H., Lee, K. J., Sung, V. M., Ishiko, H., and Lai, M. M. (2004) *Virology* **324,** 450–461
15. Egger, D., Wolk, B., Gosert, R., Bianchi, L., Blum, H. E., Moradpour, D., and Bienz, K. (2002) *J. Virol.* **76,** 5974–5984
16. Miyanari, Y., Hijikata, M., Yamaji, M., Hosaka, M., Takahashi, H., and Shimotohno, K. (2003) *J. Biol. Chem.* **278,** 50301–50308
17. Moradpour, D., Gosert, R., Egger, D., Penin, F., Blum, H. E., and Bienz, K. (2003) *Antiviral Res.* **60,** 103–109
18. Shi, S. T., Lee, K. J., Aizaki, H., Hwang, S. B., and Lai, M. M. (2003) *J. Virol.* **77,** 4160–4168
19. Watashi, K., and Shimotohno, K. (2007) *Rev. Med. Virol.* **17,** 245–252
20. Watashi, K., Hijikata, M., Hosaka, M., Yamaji, M., and Shimotohno, K. (2003) *Hepatology* **38,** 1282–1288
21. Watashi, K., Ishii, N., Hijikata, M., Inoue, D., Murata, T., Miyanari, Y., and Shimotohno, K. (2005) *Mol. Cell* **19,** 111–122
22. Goto, K., Watashi, K., Murata, T., Hishiki, T., Hijikata, M., and Shimotohno, K. (2006) *Biochem. Biophys. Res. Commun.* **343,** 879–884
23. Aly, H. H., Watashi, K., Hijikata, M., Kaneko, H., Takada, Y., Egawa, H., Uemoto, S., and Shimotohno, K. (2007) *J. Hepatol.* **46,** 26–36
24. Hino, H., Tateno, C., Sato, H., Yamasaki, C., Katayama, S., Kohashi, T., Aratani, A., Asahara, T., Dohi, K., and Yoshizato, K. (1999) *Biochem. Biophys. Res. Commun.* **256,** 184–191
25. Watashi, K., Hijikata, M., Tagawa, A., Doi, T., Marusawa, H., and Shimotohno, K. (2003) *Mol. Cell. Biol.* **23,** 7498–7509
26. Murata, T., Ohshima, T., Yamaji, M., Hosaka, M., Miyanari, Y., Hijikata, M., and Shimotohno, K. (2005) *Virology* **331,** 407–417
27. Murata, T., Hijikata, M., and Shimotohno, K. (2005) *Virology* **340,** 105–115
28. Lindenbach, B. D., Evans, M. J., Syder, A. J., Wolk, B., Tellinghuisen, T. L., Liu, C. C., Maruyama, T., Hynes, R. O., Burton, D. R., McKeating, J. A., and Rice, C. M. (2005) *Science* **309,** 623–626
29. Wakita, T., Pietschmann, T., Kato, T., Date, T., Miyamoto, M., Zhao, Z., Murthy, K., Habermann, A., Krausslich, H. G., Mizokami, M., Bartenschlager, R., and Liang, T. J. (2005) *Nat. Med.* **11,** 791–796
30. Zhong, J., Gastaminza, P., Cheng, G., Kapadia, S., Kato, T., Burton, D. R., Wieland, S. F., Uprichard, S. L., Wakita, T., and Chisari, F. V. (2005) *Proc. Natl. Acad. Sci. U. S. A.* **102,** 9294–9299
31. Shang, Y. (2006) *Nat. Rev. Cancer* **6,** 360–368
32. Callaghan, R., and Higgins, C. F. (1995) *Br. J. Cancer* **71,** 294–299
33. Raderer, M., and Scheithauer, W. (1993) *Cancer* **72,** 3553–3563
34. Lopes, M. C., Vale, M. G., and Carvalho, A. P. (1990) *Cancer Res.* **50,** 2753–2758
35. O'Brian, C. A., Liskamp, R. M., Solomon, D. H., and Weinstein, I. B. (1985) *Cancer Res.* **45,** 2462–2465
36. O'Brian, C. A., Ward, N. E., and Anderson, B. W. (1988) *J. Natl. Cancer Inst.* **80,** 1628–1633
37. Leers, J., Treuter, E., and Gustafsson, J. A. (1998) *Mol. Cell. Biol.* **18,** 6001–6013
38. Schmidt-Mende, J., Bieck, E., Hugle, T., Penin, F., Rice, C. M., Blum, H. E., and Moradpour, D. (2001) *J. Biol. Chem.* **276,** 44052–44063
39. Evans, M. J., Rice, C. M., and Goff, S. P. (2004) *Proc. Natl. Acad. Sci. U. S. A.* **101,** 13038–13043
40. Gao, L., Aizaki, H., He, J. W., and Lai, M. M. (2004) *J. Virol.* **78,** 3480–3488
41. Wang, C., Gale, M., Jr., Keller, B. C., Huang, H., Brown, M. S., Goldstein, J. L., and Ye, J. (2005) *Mol. Cell* **18,** 425–434

42. Kapadia, S. B., and Chisari, F. V. (2005) *Proc. Natl. Acad. Sci. U. S. A.* **102,** 2561–2566
43. Ye, J., Wang, C., Sumpter, R., Jr., Brown, M. S., Goldstein, J. L., and Gale, M., Jr. (2003) *Proc. Natl. Acad. Sci. U. S. A.* **100,** 15865–15870
44. Migliaccio, A., Piccolo, D., Castoria, G., Di Domenico, M., Bilancio, A., Lombardi, M., Gong, W., Beato, M., and Auricchio, F. (1998) *EMBO J.* **17,** 2008–2018
45. Razandi, M., Pedram, A., Greene, G. L., and Levin, E. R. (1999) *Mol. Endocrinol.* **13,** 307–319
46. Wyckoff, M. H., Chambliss, K. L., Mineo, C., Yuhanna, I. S., Mendelsohn, M. E., Mumby, S. M., and Shaul, P. W. (2001) *J. Biol. Chem.* **276,** 27071–27076

Available online at www.sciencedirect.com
ScienceDirect
Virology 365 (2007) 285–291
VIROLOGY
www.elsevier.com/locate/yviro

Influences on hepatitis B virus replication by a naturally occurring mutation in the core gene☆

Masaya Sugiyama [a], Yasuhito Tanaka [a], Fuat Kurbanov [a], Nobuaki Nakayama [b], Satoshi Mochida [b], Masashi Mizokami [a,*]

[a] *Department of Clinical Molecular Informative Medicine, Nagoya City University Graduate School of Medical Sciences, Kawasumi, Mizuho, Nagoya 467-8601, Japan*
[b] *Division of Gastroenterology and Hepatology, Internal Medicine, Saitama Medical University, 38 Morohongo, Moroyama-cho, Iruma-gun, Saitama 350-0495, Japan*

Received 17 November 2006; returned to author for revision 10 January 2007; accepted 7 April 2007
Available online 10 May 2007

Abstract

Little is known about specific naturally occurring mutations of hepatitis B virus (HBV) and underlying mechanisms of their association with fulminant hepatitis. A HBV clone isolated from a patient with fulminant hepatitis was analyzed, and the features of the particular mutations observed around furin cleavage site in core region (A2339G/G2345A) were assessed using an *in vitro* replication model. The clone belonged to genotype B with precore stop codon mutation (G1896A). Replication efficiency of 1.24-fold HBV genome in Huh-7 cells was increased in the presence of A2339G. Further *in vitro* studies using furin inhibitor indicated that the effect of the mutation was probably associated with accumulation of the full-length core protein without cleavage by furin-like protease, suggesting that a processing of the core protein might play an important role in regulation of viral replication. In conclusion, the A2339G mutation was considered as one of the viral factors involved in high replication efficiency.

Keywords: Hepatitis B virus; Core protein; Genotype; Furin; Fulminant hepatitis; Replication

Introduction

Hepatitis B virus (HBV) remains a major human pathogen. Although new infections are preventable through vaccination, new antiviral targets are being sought for the treatment of the estimated 350 million affected individuals worldwide (Lee, 1997). While acute infection with HBV resolves in the great majority of patients, in a proportion of patients HBV can induce fulminant hepatitis or go on to become chronic hepatitis. What factors influence the fulminant or chronic outcome of acute HBV infection are not fully defined. Approximately 10% of adults and 90% of children become persistent HBV carriers after HBV infection, and 1–2 million people die annually as the consequence of infection with the virus, due to liver cirrhosis and hepatocellular carcinoma.

HBV is the prototype strain of the family *Hepadonaviridea*. The virus has an approximately 3.2 kb circular, double-stranded DNA genome with four open reading frames: core (C), polymerase (P), surface (S), and X. Eight genotypes have been detected with a sequence divergence greater than 8% in the entire HBV genome (Okamoto et al., 1988) and been designated by capital alphabet letters from A (HBV/A) to H (HBV/H) in the order of their discovery (Arauz-Ruiz et al., 2002; Norder et al., 1994; Stuyver et al., 2000). The genotypes have distinct geographical distributions and are associated with differing severities of liver disease as well as response to antiviral therapies (Chu and Lok, 2002; Kao, 2002; Miyakawa and Mizokami, 2003).

The core region encodes two gene products, core protein and HBe antigen (HBeAg), translated from two different transcripts of 3.5 and 3.6 kb, respectively; the differences of the two products were; however, only the amino acids at the N-terminus. Most of the synthetic pathway of HBeAg is now clearly established. In 2003, Messageot and colleagues reported

☆ The nucleotide sequence of HBV-DNA isolates used in this study has been deposited in the international DNA database under accession number AB302095.

* Corresponding author. Fax: +81 52 842 0021.
E-mail address: mizokami@med.nagoya-cu.ac.jp (M. Mizokami).

0042-6822/$ - see front matter © 2007 Elsevier Inc. All rights reserved.
doi:10.1016/j.virol.2007.04.004

that the C-terminal extremity of HBeAg was located at position 154 and that a proprotein convertase, furin, was involved in the maturation (Messageot et al., 2003).

Furin or furin-like protease is a transmembrane proprotein convertase localized in the *trans*-Golgi network (TGN), transported to the plasma membrane and then retrieved back through the endocytic pathway (Molloy et al., 1999). The consensus sequence of the furin cleavage site is RXK/RR, which has strictly required arginine residues at both the head and tail of the cleavage site (Nakayama, 1997). The furin cleavage site of the HBeAg C-terminus was reported as ^{151}RRGR^{154} (Fig. 1) (Messageot et al., 2003). Therefore, their results strongly indicate that the secretory HBeAg ends at Arg^{154}.

Recently, a patient was referred to our hospital for developing fulminant hepatitis B. Sequence analysis of the causal HBV revealed naturally occurring A2339G and G2345A mutations in the core region, and harboring the precore stop codon G1896A mutation. The replication efficiency *in vitro* of these clones was significantly higher than other clones with the G1896A mutation, which had been constructed before (unpublished data). The novel mutations may be responsible for the higher replication efficiency since the region of the mutation sites is adjacent to the furin cleavage site. To elucidate the biological properties of naturally occurring mutations, although the synthetic and secretory pathways of the core protein are not completely understood, we investigated whether the A2339G and/or G2345A mutations influence viral replication following transient transfection into human hepatoma cell lines.

Results

Influence of A2339G on HBV replication

A serum sample was obtained from a patient with fulminant hepatitis, in whom prothrombin time decreased less than 40% of the controls with hepatic encephalopathy of grade II or more within 8 weeks after the onset of the disease. The results of sequence analysis revealed unique mutation, A2339G and G2345A, in core gene. Then, we constructed plasmids with or without mutations and examined virological characteristics (Fig. 1). Huh-7 cells were transfected in 10-cm dish with 5 μg of each plasmid and harvested 2 days posttransfection. Southern blot analysis of core-associated HBV DNA in the cell lysate demonstrated that transfection of both pBj_2339 and pBj_2339/45 showed approximately 1.4-fold increase of core-associated HBV DNA as compared to the pBj_wild construct (Fig. 2A), while the transfection of pBj_2345 construct did not reveal the different result from wild type. The difference between these plasmids resides only in the mutations present in the core gene, as shown in Fig. 1. The transfection efficiency was monitored by reporter plasmids expressing secreted alkaline phosphatase (SEAP). But the correction of the transfection efficiency was not performed because each experiment in this study showed almost equal value. For immunoblot analysis, a particular monoclonal antibody was adopted. Because the anti-core protein monoclonal antibodies (HB50) recognize SPRRR repeats in the arginine-rich domain of core protein, only the full-length core protein, which is not cleaved by furin-like protease, can be detected by the HB50 antibody. Immunoblot analysis of cell lysate revealed approximately 1.3-fold increase of the core protein in pBj_2339 and pBj_2339/45 transfection (Fig. 2A) as compared to pBj_wild and pBj_2345, indicating that the A2339G mutation could be associated with the high expression of the core protein. This was not due to larger amounts of sample of the A2339G mutants, as revealed by reprobing of the same blot with anti-α-tubulin antibodies (lower panel in Figs. 2A and B). Transfection efficiency was monitored by cotransfection with a gene encoding SEAP. These results were confirmed by at least three replicates. Additionally, similar results were also obtained when these clones were used for transfection of HepG2 cells (data not shown).

The A2339G mutation obstructed the function of a cellular proprotein convertase

Precore proprotein undergoes enzymatic maturation by a protease activated both in the post-endoplasmic reticulum compartment and at the cell surface, which is a well known

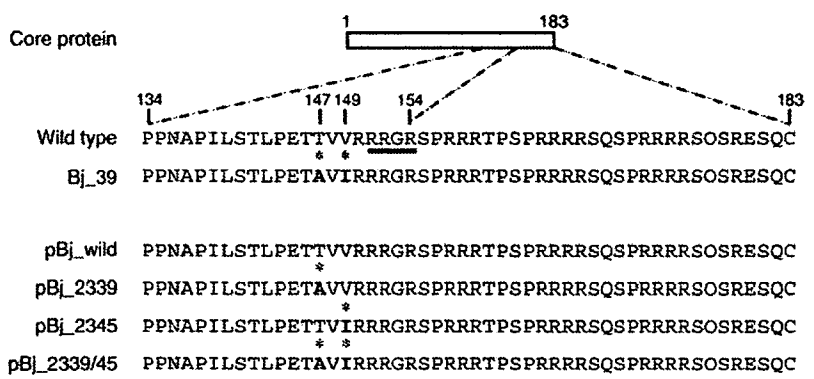

Fig. 1. C-terminus amino acid sequences and substitution mutants of the core protein. The ORF contains two in-frame initiation codons, delimiting the precore sequence and the C gene. Conventionally, position number 1 is assigned to the first amino acid of the core protein. As reported previously by Messageot *et al.*, the C-terminus of the precore protein ends at Arg^{154}. The amino acid of the putative furin cleavage site is underlined. The wild-type sequence of the core protein is shown on the upper line. Names of all of the substitution mutants referred to in this paper are on the left. In each case the corresponding sequence is shown, with the mutation indicated in bold and with an asterisk.

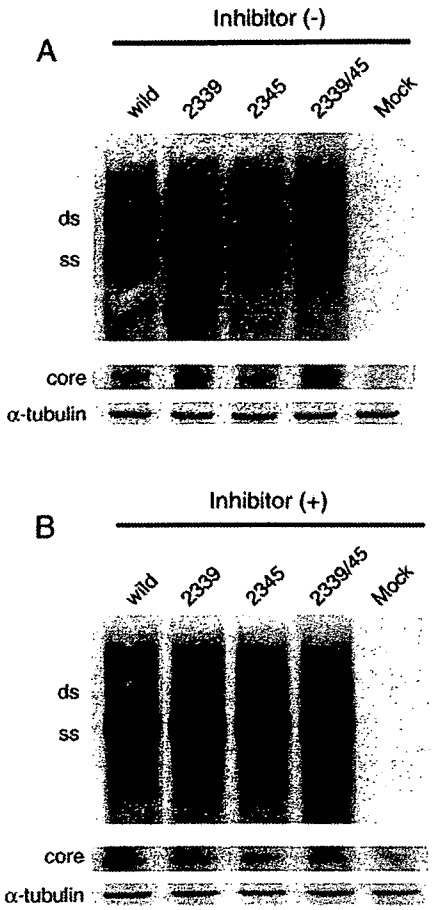

Fig. 2. Replication of the A2339G and/or G2345A mutants with or without 20 μM furin specific inhibitor, decanoyl-RVKR-chloromethylketone (dec-RVKR-cmk). Southern blot analysis of intracellular HBV replication. Isolated core-associated HBV DNAs were separated on a 1.2% agarose gel. Immunoblot analysis of core protein expression from the various constructs was performed by using HB50 monoclonal antibody. The blots were stripped of the antibodies and reprobed with a mouse anti-α-tublin antibody. (A) Without the specific inhibitor. (B) With 20 μM specific inhibitor. These results were confirmed by at least three replicates. ss: single strand DNA, ds: double strand DNA.

characteristic of furin. As the ORF of the core protein C-terminus is the same as the precore proprotein, core protein might have a similar processing step by furin. To determine whether furin-like protease is the protease involved in core maturation, a specific inhibitor, decanoyl-RVKR-chloromethylketone (dec-RVKR-cmk), was used in the next experiment. The inhibitor, at a concentration of 20 μM, was added into the medium and was maintained through to the cell lysis stage. As shown in Fig. 2B, under these conditions, the replication levels of pBj_wild and pBj_2345 became quite equal to pBj_2339 and pBj_2339/45. The expression levels of the core protein were not different between each plasmid (Fig. 2B). Thus, inhibition of the proteolytic activity of furin could induce the increase of both HBV replication and core protein expression, indicating that this protease is involved in the processing pathway of the core protein.

Influence on the replication capacities by the amount of core protein

As the replication capacity correlated well with the expression levels of core protein (Fig. 2), it would be insufficient to analyze the influence of the core protein on replication efficiency using the above replication model. To determine whether the core protein harboring the A2339G mutation avoids processing by furin-like protease, we generated expression plasmids encoding the core gene only. These plasmids drive the synthesis of wild type, A2339G, G2345A, or A2339G/G2345A core protein from the cytomegalovirus promoter, which were named pcDNA/core_wild, core_2339, core_2345, and core_2339/45, respectively. Transient expression of the core protein was achieved by transfection of Huh-7 cells with these plasmids. The transfection efficiency was monitored by SEAP. Immunoblot analysis showed higher expression levels of the uncleaved core protein for core_2339 and core_2339/45 than that for core_wild and core_2345 in conditions without furin inhibitor (Fig. 3A). In contrast, in the presence of the furin inhibitor, the amounts of full-length core protein were equal between each of the plasmid (Fig. 3B). These results were consistent with those from experiments using the 1.24-fold HBV genome as shown in Fig. 2; the A2339G mutation may enhance full-length core protein expression as well as viral replication due to the inhibition of core protein processing by furin-like protease.

No influence of furin against core protein processing

It is well-known that furin inhibitor has the ability to inhibit some proteases. To specifically silence furin, we designed

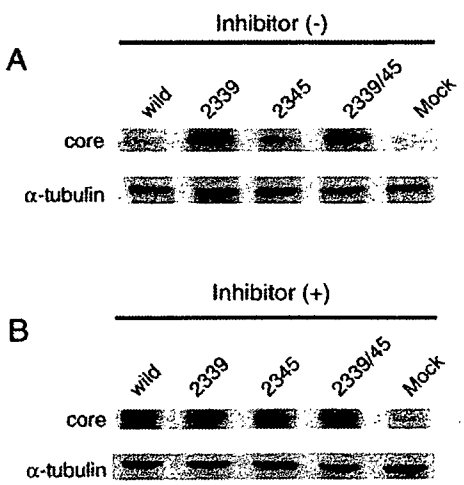

Fig. 3. Immunoblot analysis of core protein expression by the mutants expressing the core gene only. Huh-7 cells were transfected with both pcDNA/core expression vector and reporter plasmid with SEAP, and harvested 2 days posttransfection. Immunoblot analysis was performed to determine the expression levels of core protein and α-tubulin by HB50 (anti-core monoclonal antibody) and anti-α-tubulin monoclonal antibody, respectively. (A) Samples were collected from transfected cells cultured in the inhibitor-free medium. (B) Cell lysates were prepared for analysis at a concentration of 20 μM dec-RVKR-cmk.